Acetylation of Dendrimer-Entrapped Gold Nanoparticles: Synthesis, Stability, and X-ray Attenuation Properties

Chen Peng,[1,2] Han Wang,[3] Rui Guo,[2] Mingwu Shen,[2] Xueyan Cao,[2] Meifang Zhu,[1] Guixiang Zhang,[3] Xiangyang Shi[1,2]

[1]*State Key Laboratory for Modification of Chemical Fibers and Polymer Materials, Donghua University, Shanghai 201620, People's Republic of China*
[2]*College of Chemistry, Chemical Engineering and Biotechnology, Donghua University, Shanghai 201620, People's Republic of China*
[3]*Department of Radiology, Shanghai First People's Hospital, Medical College, Shanghai Jiaotong University, Shanghai 200080, People's Republic of China*

Received 19 February 2010; accepted 23 May 2010
DOI 10.1002/app.32845
Published online 19 August 2010 in Wiley Online Library (wileyonlinelibrary.com).

ABSTRACT: Functionalized dendrimer-entrapped gold nanoparticles (Au DENPs) are of scientific and technological interest in biomedical applications. In this study, Au DENPs prepared with amine-terminated generation 5 (G5) poly(amido amine) dendrimers as templates were subjected to acetylation to neutralize the positive surface charge of the particles. By varying the molar ratio of Au salt to G5 dendrimer, we prepared acetylated Au DENPs with a size range of 2–4 nm. Meanwhile, we attempted to add glucose to the dialysis liquid of the acetylated Au DENPs to prevent possible particle aggregation after lyophilization. The acetylated Au DENPs with different compositions (Au salt/dendrimer molar ratios) were characterized with ^{1}H-NMR, transmission electron microscopy, ultraviolet–visible (UV–vis) spectrometry, and ζ-potential measurements. We show that when the molar ratio of Au salt to dendrimer was equal to or larger than 75:1, the acetylated Au DENPs showed a significant aggregation after lyophilization, and the addition of glucose was able to preserve the colloidal stability of the particles. X-ray absorption measurements showed that the attenuation of the acetylated Au DENPs was much higher than that of the iodine-based contrast agent at the same molar concentration of the active element (Au vs iodine). In addition, the acetylated Au DENPs enabled X-ray computed tomography (CT) imaging of mice after intravenous injection of the particles. These findings suggest a great potential for acetylated Au DENPs as a promising contrast agent for CT imaging applications. © 2010 Wiley Periodicals, Inc. J Appl Polym Sci 119: 1673–1682, 2011

Key words: dendrimers; imaging; nanocomposites; nanoparticle

INTRODUCTION

As one of the most attractive nanomaterials, gold nanoparticles (Au NPs) have recently received immense scientific and technological interest for their extensive applications in biology, catalysis, and nanotechnology because of their unique optical, electronic, and quantum size-related properties.[1–9] In particular, for biomedical applications, Au NPs have been intensively used in cancer-cell imaging and photothermal therapy,[10–14] which is largely because of their unique light-scattering properties and biocompatibility.[15,16] In most of these applications, the Au NP surfaces have to be modified with different functionalities.[17,18]

One unique approach to the preparation of Au NPs is through the use of poly(amido amine) (PAMAM) dendrimers as templates.[2,19–26] PAMAM dendrimers are a class of highly branched, monodispersed, synthetic macromolecules with well-defined structures and compositions.[27,28] With PAMAM dendrimers as templates, dendrimer-entrapped gold nanoparticles (Au DENPs) can be formed with each Au NP entrapped within each dendrimer

Correspondence to: X. Shi (xshi@dhu.edu.cn) or G. Zhang (guixiangzhang@sina.com).

Contract grant sponsor: National Natural Science Foundation of China; contract grant numbers: 20974019, 30901730, and 50925312.
Contract grant sponsor: National Basic Research Program of China (973 Program); contract grant number: 2007CB936000.
Contract grant sponsor: Shanghai Pujiang Program; contract grant number: 09PJ1400600.
Contract grant sponsor: Program for Professor of Special Appointment (Eastern Scholar) at Shanghai Institutions of Higher Learning.
Contract grant sponsor: Fundamental Research Funds for the Central Universities (for R.G., M.S., X.C., and X.S.).
Contract grant sponsor: Young Teacher Foundation of Donghua University (for R.G.); contract grant number: 200802.
Contract grant sponsor: Shanghai Natural Science Foundation (for R.G.); contract grant number: 10ZR1400800.
Contract grant sponsor: Ph.D. Programs Foundation of Ministry of Education of China (for G.Z.); contract grant number: 20090073110072.

molecule.[22,23] The advantage of using dendrimers as templates to prepare Au NPs lies in the fact that the surface of the particles can be modified with various functional moieties (e.g., targeting ligands and dyes) through dendrimer chemistry for practical biomedical applications (e.g., cancer-cell targeting and imaging).[22,29,30] For instance, Au DENPs with a size of 2 nm prepared with amine-terminated generation 5 PAMAM dendrimers (G5.NH_2's) can be modified with folic acid and fluorescein isothiocyanate for the subsequent targeting and imaging of cancer cells overexpressing high-affinity folic acid receptors.[22] Arginine-glycine-aspartic acid (RGD) peptide-functionalized generation 5 (G5) dendrimers can be used as templates to form Au DENPs with a size of 3 nm, which can specifically target tumor vasculature-related endothelial cells overexpressing $\alpha V\beta 3$ integrin.[30] These studies have clearly indicated that PAMAM dendrimers are promising templates for the generation of multifunctional Au DENP-based nanoplatforms for various biomedical applications. One of the key steps in the preparation of Au DENPs for ready use for biological applications is the rendering of the particle surface charge to neutral. This can be achieved by the acetylation of dendrimer terminal amines.[21–23,31] Our previous work[21,23] has shown that Au DENPs formed with G5.NH_2 dendrimers as templates with an Au salt/dendrimer molar ratio of 51.2:1 can be acetylated to render particles with a similar size and size distribution to those before acetylation. The acetylated Au DENPs, having neutral surface charges, are water soluble, colloidally stable, and biocompatible at a concentration up to 2 μM.

As is generally known, the driving force to render Au DENPs prepared with amine-terminated dendrimers as templates colloidally stable is believed to be the interaction between the dendrimer terminal/tertiary amines and the Au NP surfaces.[2,23,32] In the case of Au DENPs (Au salt/dendrimer molar ratio = 51.2 : 1) in our previous work,[21,23] after acetylation, the tertiary amines of G5 dendrimers gave stabilization to the Au DENPs. For acetylated Au DENPs, the stabilization force of dendrimer tertiary amines is expected to be limited when the entrapped Au NPs have a slightly larger size prepared with larger Au salt/dendrimer molar ratios.

Recently, Au NPs have been used as contrast agents for X-ray computed tomography (CT) imaging because of their strong X-ray attenuation characteristics, biocompatibility, and easy surface functionalization ability compared with conventional iodine-based CT contrast agents.[33–37] In a previous report, we demonstrated that Au DENPs with a size range of 2–4 nm could be prepared with G5.NH_2 as templates by the variation of the Au salt/dendrimer molar ratio from 25 : 1 to 200 : 1, and the X-ray attenuation properties of the Au DENPs did not change significantly within the Au DENP size range.[26] However, because of the abundant amine groups present in the Au DENPs prepared with G5.NH_2 dendrimer templates, this material displayed nonspecific binding with cell membranes and cytotoxicity at high concentrations; this, thereby, limits their further biomedical applications.

In this study, we systematically investigated the effect of acetylation on the stability of Au DENPs with a size range of 2–4 nm prepared with different Au salt/dendrimer molar ratios. To prevent the possible particle aggregation during lyophilization, we attempted to add glucose as a protecting agent to the dialysis liquid of the acetylated Au DENP solution. The acetylated Au DENPs were characterized with ^{1}H-NMR, ζ-potential measurements, UV–vis spectrometry, and transmission electron microscopy (TEM). In addition, X-ray absorption coefficient measurements were performed to examine the X-ray attenuation properties of these particles. The acetylated Au DENPs were further intravenously injected into mice to evaluate the *in vivo* CT imaging capabilities. To our knowledge, this is the first report relating to the effect of the storage/processing conditions on the stability of acetylated Au DENPs with different Au salt/dendrimer molar ratios. Findings from this study will contribute to the rational design of Au DENP-based contrast agents for CT imaging applications.

EXPERIMENTAL

Materials

Ethylenediamine core G5.NH_2's with a polydispersity index of less than 1.08 were purchased from Dendritech (Midland, MI). All other chemicals were obtained from Aldrich (St. Louis, MO) and were used as received. The water used in all of the experiments was purified with a Milli-Q Plus 185 water purification system (Millipore, Bedford, MA) with a resistivity higher than 18 MΩ cm. Regenerated cellulose dialysis membranes (molecular weight cutoff = 10,000) were acquired from Fisher (Waltham, MA).

Synthesis sand acetylation of the Au DENPs

The procedure that we used to synthesize Au DENPs was adopted from previously reported methods.[23,26] The Au DENPs were prepared with sodium borohydride reduction chemistry with molar ratios of Au salt to the dendrimer of 25 : 1, 50 : 1, 75 : 1, 100 : 1, 125 : 1, and 150 : 1, respectively. Briefly, a certain amount of $HAuCl_4$ solution [2.5 mL in water/methanol (v/v = 2 : 1)] was added to an aqueous solution of G5.NH_2 (20 mg, 10 mL) under vigorous stirring. After 30 min, an icy cold $NaBH_4$

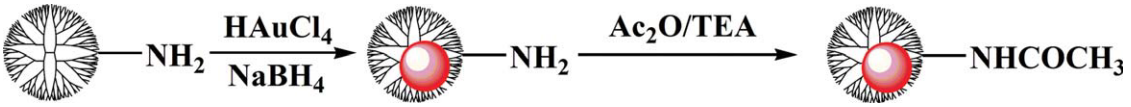

Scheme 1 Schematic illustration of the preparation of the $(Au^0)_n$-G5.NHAc DENPs. Ac_2O and TEA represents acetic anhydride and triethylamine, respectively. [Color figure can be viewed in the online issue, which is available at wileyonlinelibrary.com.]

solution [5 mL in water/methanol (v/v = 2 : 1)] with a three times molar excess to the Au salt was added to the Au salt/dendrimer mixture under stirring, and the reaction mixture turned a deep red color within a few seconds. The stirring process was continued for 2 h to complete the reaction. The reaction mixture was then extensively dialyzed against water (six times, 4 L) for 3 days to remove the excess reactants; this was followed by lyophilization to obtain the Au DENPs. The final Au DENP products are denoted as $(Au^0)_n$-G5.NH_2, where n = 25, 50, 75, 100, 125, and 150, respectively.

The $(Au^0)_n$-G5.NH_2 DENPs were further acetylated to neutralize the dendrimer terminal amine groups. Briefly, triethylamine (54.7 μL) was added to an aqueous solution of $(Au^0)_n$-G5.NH_2 DENPs (25 mL, 21.12 mg) under magnetic stirring. After 30 min, acetic anhydride (31.0 μL, 324 m*M*, 400% molar excess of the total primary amines of Au DENPs) was added to the DENP/triethylamine mixture solution with stirring, and the mixture was allowed to react for 24 h. The aqueous solution of the reaction mixture was extensively dialyzed against phosphate buffered saline (PBS) buffer (three times, 4 L) and water (three times, 4 L) for 3 days to remove excess reactants and byproducts. The dialysis liquid was divided into three aliquots with equal volumes. The first aliquot was kept at 4°C. The second aliquot was lyophilized directly. The third aliquot was added with glucose with an Au DENP/glucose mass ratio of 1 : 5 and then lyophilized.

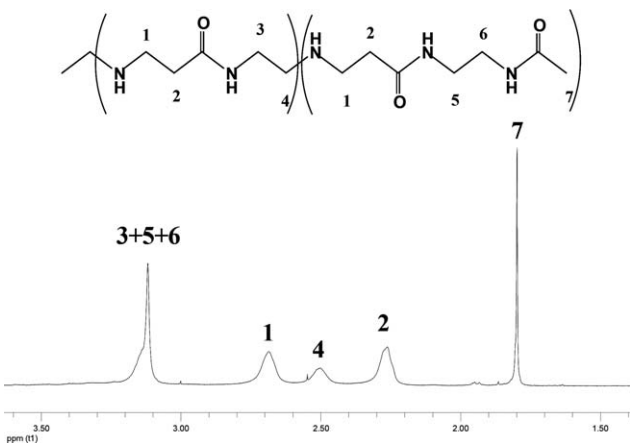

Figure 1 ^{1}H-NMR spectrum of the $(Au^0)_{50}$-G5.NHAc DENPs.

Characterization techniques

UV–vis spectra were collected with a Lambda 25 UV–vis spectrometer (Perkin Elmer, Norwalk, CT). Samples were dissolved in water before the experiments. TEM was performed with a JEOL 2010F analytical electron microscope (JEOL, Tokyo, Japan) operating at 200 kV. An aqueous solution of Au DENPs (1 mg/mL) was dropped onto a carbon-coated copper grid and air-dried before measurements. The size distribution histogram of Au DENPs was analyzed with ImageJ software (http://rsb.info.nih.gov/ij/download.html, NIH, Bethesda, MD). For each sample, 300 NPs were randomly selected to analyze the size. ζ-potential measurements were carried out with a Zetasizer Nano ZS system (Malvern, Worcestershire, United Kingdom) equipped with a standard 633-nm laser.

Micro-CT imaging

Acetylated Au DENPs and the clinically used CT agent iohexol 300 (Omnipaque, 300 mg of I/mL, GE Healthcare, Fairfield, CT) solutions with different concentrations were prepared in 0.2-mL Axygen polymerase chain reaction (PCR) tubes and placed in a self-designed scanning holder. CT scans were performed with a micro-CT imaging system (eXplore

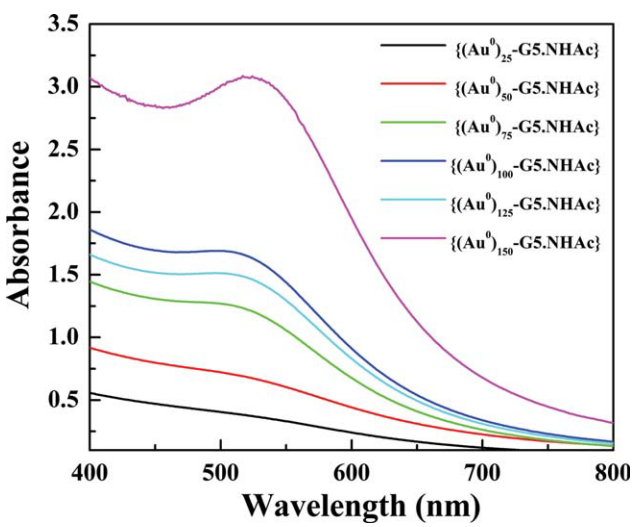

Figure 2 UV–vis spectra of acetylated Au DENPs formed with different Au salt/dendrimer molar ratios. [Color figure can be viewed in the online issue, which is available at wileyonlinelibrary.com.]

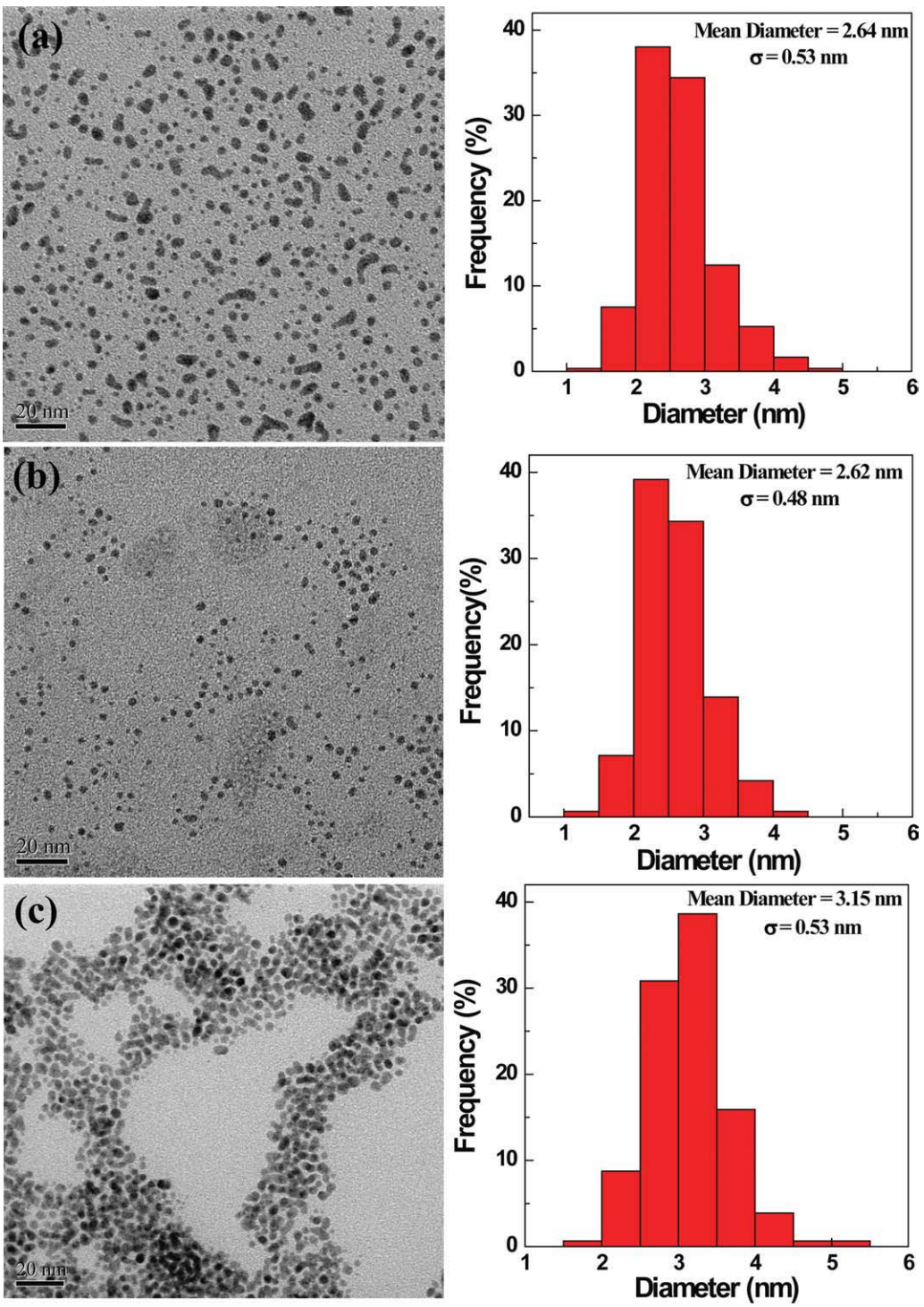

Figure 3 TEM images and size distribution histograms of the freshly prepared (a) $(Au^0)_{50}$-G5.NHAc, (b) $(Au^0)_{100}$-G5.NHAc, and (c) $(Au^0)_{150}$-G5.NHAc DENPs without lyophilization. σ represents standard deviation. [Color figure can be viewed in the online issue, which is available at wileyonlinelibrary.com.]

Locus, GE, Fairfield, CT) at 80 kV and 45 μA and with a slice thickness of 45 μm. Evaluation of the contrast enhancement of the $(Au^0)_n$-G5.NHAc (NHAc denotes $NHCOCH_3$) DENPs was carried out by the loading of the digital CT images in a standard display program and, then, the selection of a uniform round region of interest on the resulting CT image for each sample. Contrast enhancement was determined in Hounsfield units for each concentration of $(Au^0)_n$-G5.NHAc DENPs with different compositions and Omnipaque.

Imprinting control region (ICR) mice (20–25 g, Shanghai Laboratory Animal Center, Shanghai, China) were anesthetized by intraperitoneal injection

of 0.3 mL of 3% pentobarbital sodium (12 mL/kg). $(Au^0)_{50}$-G5.NHAc DENPs (2.5 μmol of Au/g of body weight) dispersed in PBS buffer were then injected into the mice through the tail vein. Two minutes later, the mice were scanned by a micro-CT imaging system with a tube voltage of 80 kV, an electrical current of 450 μA, and a slice thickness of 45 μm. Images were reconstructed by GEHC microView software (GE, Fairfield, CT) on the basis of voxels of $45 \times 45 \times 45$ μm^3. For a control experiment, Omnipaque with a similar iodine concentration was injected into the mice, and CT scanning was performed under similar conditions.

RESULTS AND DISCUSSION

Acetylation of the Au DENPs

$G5.NH_2$ dendrimers were used as templates to generate Au DENPs with different Au salt/dendrimer molar ratios. The formed Au DENPs were further acetylated to neutralize the dendrimer terminal amines (Scheme 1). The obtained $(Au^0)_n$-G5.NHAc DENPs were characterized with ^{1}H-NMR. Figure 1 shows the ^{1}H-NMR spectrum of the $(Au^0)_{50}$-G5.NHAc DENPs, which was similar to that of the acetylated G5 dendrimers.[31] The acetylated Au DENPs prepared with other Au salt/dendrimer molar ratios displayed similar ^{1}H-NMR spectra. This suggests that the entrapped Au NPs did not impact the transformation of the dendrimer terminal amines to acetyl groups; this was in agreement with the literature.[23]

The optical properties of the freshly prepared acetylated Au DENPs were investigated with UV–vis spectrometry (Fig. 2). It was clear that all of acetylated Au DENPs except $(Au^0)_{150}$-G5.NHAc displayed a surface plasmon resonance (SPR) peak around 510 nm, in agreement with literature.[23] The SPR peak shifted to 523 nm for the case of $(Au^0)_{150}$-G5.NHAc, presumably because of the increased size of the particles prepared with a larger Au salt/dendrimer molar ratio.

The size and morphology of the formed $(Au^0)_n$-G5.NHAc DENPs were characterized with TEM. Figure 3 shows the TEM images and size distribution histograms of freshly prepared $(Au^0)_{50}$-G5.NHAc, $(Au^0)_{100}$-G5.NHAc, and $(Au^0)_{150}$-G5.NHAc DENPs without lyophilization, respectively. It was clear that the size of Au NPs at a given Au salt/dendrimer molar ratio fell within a relatively narrow range at 2–4 nm. Even when the Au salt/dendrimer molar ratio was as high as 150:1, the mean size of $(Au^0)_{150}$-G5.NHAc was still smaller than 4 nm; this suggested that the formation and growth of the Au NPs were effectively restricted within the PAMAM dendrimer templates, and the acetylation reaction did not significantly affect the size of Au DENPs compared with those of the Au DENPs before acetylation.[23,26]

TABLE I
ζ Potential Values of $(Au^0)_n$-G5.NHAc DENPs Prepared with Different Au Salt/Dendrimer Molar Feeding Ratios

Sample	ζ potential (mV)
$(Au^0)_{25}$-G5.NHAc DENPs	3.28 ± 0.24
$(Au^0)_{50}$-G5.NHAc DENPs	3.91 ± 0.30
$(Au^0)_{75}$-G5.NHAc DENPs	5.37 ± 0.21
$(Au^0)_{100}$-G5.NHAc DENPs	9.13 ± 0.31
$(Au^0)_{125}$-G5.NHAc DENPs	10.53 ± 3.35
$(Au^0)_{150}$-G5.NHAc DENPs	14.23 ± 0.84

The formed $(Au^0)_n$-G5.NHAc DENPs prepared with different Au salt/dendrimer molar ratios had slightly positive surface potentials in the range of 3.28–14.23 mV (Table I), which were significantly lower than those of the Au DENPs before acetylation.[23] This further confirmed the successful acetylation reaction to transform the dendrimer terminal amine groups to acetyl groups. The slightly positive surface potentials of the acetylated Au DENPs were ascribed to an incomplete acetylation reaction.[23,31] With increasing Au salt/dendrimer molar ratio, the ζ potential of the acetylated Au DENPs increased slightly.

Stability of the acetylated Au DENPs

The stability of the $(Au^0)_n$-G5.NHAc DENPs could greatly affect their further biological applications. Therefore, the optimization of the storage and processing conditions of acetylated Au DENPs is of paramount importance. In general, for biomedical applications, it would be ideal if the particles after lyophilization could be redispersed into water and have similar properties to those before lyophilization. Freshly prepared acetylated Au DENPs in dialysis liquids are stable enough and allow us to characterize them with different techniques. However, the lyophilized $(Au^0)_n$-G5.NHAc DENPs prepared with an Au salt/dendrimer molar ratio of 75 : 1 or greater could be redispersed into water, but a portion of the particles precipitated after 10–20 min. This was in sharp contrast to the Au DENPs prepared with an Au salt/dendrimer molar ratio in the range 25 : 1–200 : 1 before the acetylation reaction, which showed great stability in the pH range 5–8 and the temperature range 4–50°C after lyophilization.[26] We believe that the lyophilization process could significantly shorten the interparticle distance and promote particle aggregation. For the Au DENPs before acetylation, the abundant dendrimer terminal amines were able to stabilize the Au NPs and preserve the good colloidal stability of the particles after redispersion into water. However, for

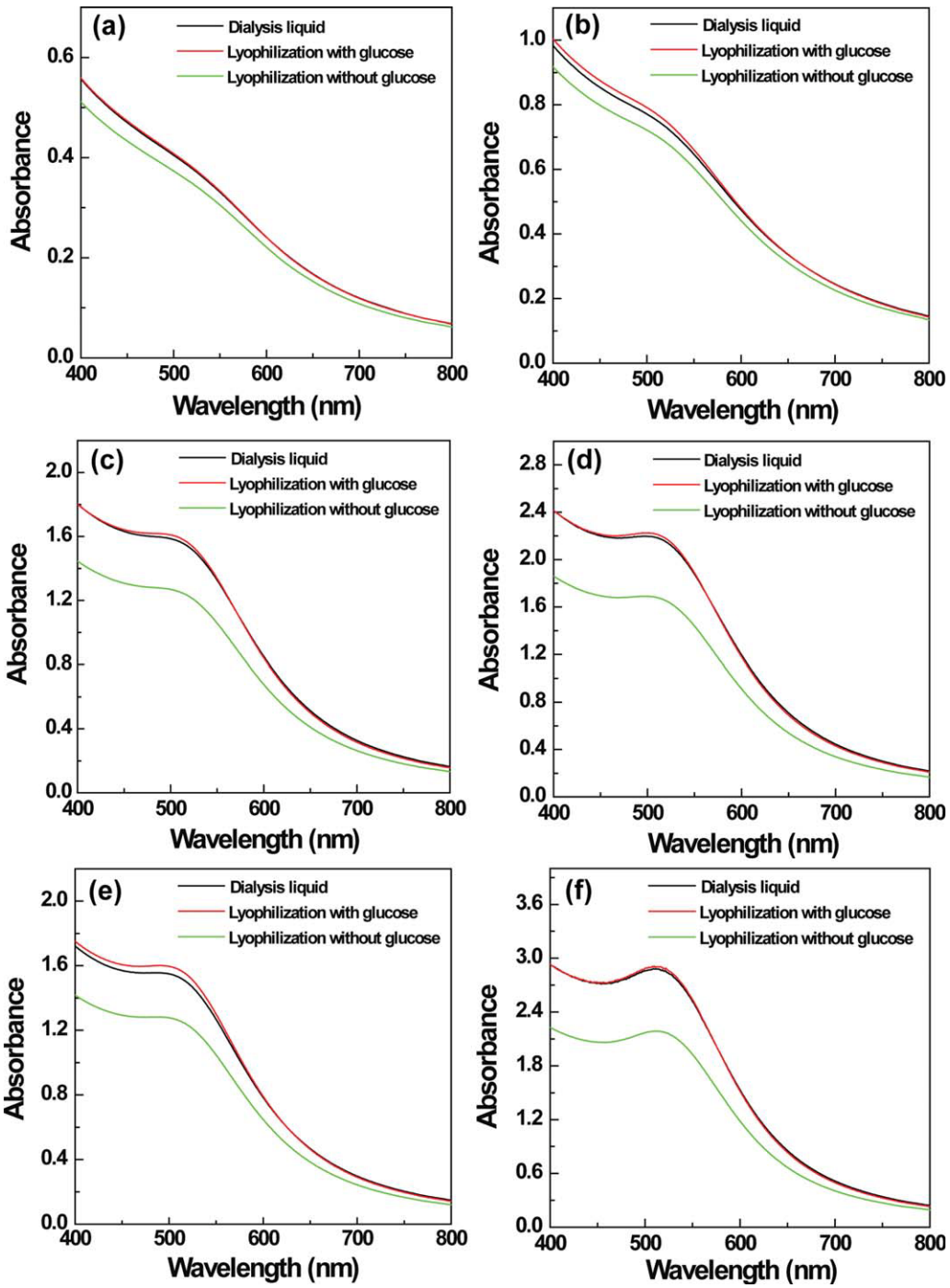

Figure 4 UV–vis spectra of $(Au^0)_n$-G5.NHAc DENPs prepared with different Au salt/dendrimer molar ratios [n = (a) 25, (b) 50, (c) 75, (d) 100, (e) 125, and (f) 150] under different conditions: stored in dialysis liquid, directly lyophilized, and then redispersed in water and lyophilized with the protecting agent glucose and then redispersed in water. [Color figure can be viewed in the online issue, which is available at wileyonlinelibrary.com.]

acetylated Au DENPs prepared with larger Au salt/dendrimer molar ratios, because of the lack of dendrimer primary amine stabilization, the lyophilization process decreased the colloidal stability after the particles were redispersed into water. Hence, in this study, we attempted to preserve the redispersion colloidal stability of $(Au^0)_n$-G5.NHAc DENPs by adding glucose to the dialysis liquids of the particles before lyophilization.

Literature data show that the changes in the UV–vis absorption characteristics can effectively reflect the aggregation degree of Au NPs.[38] Therefore, in our study, the stability of the $(Au^0)_n$-G5.NHAc DENPs under different conditions was evaluated

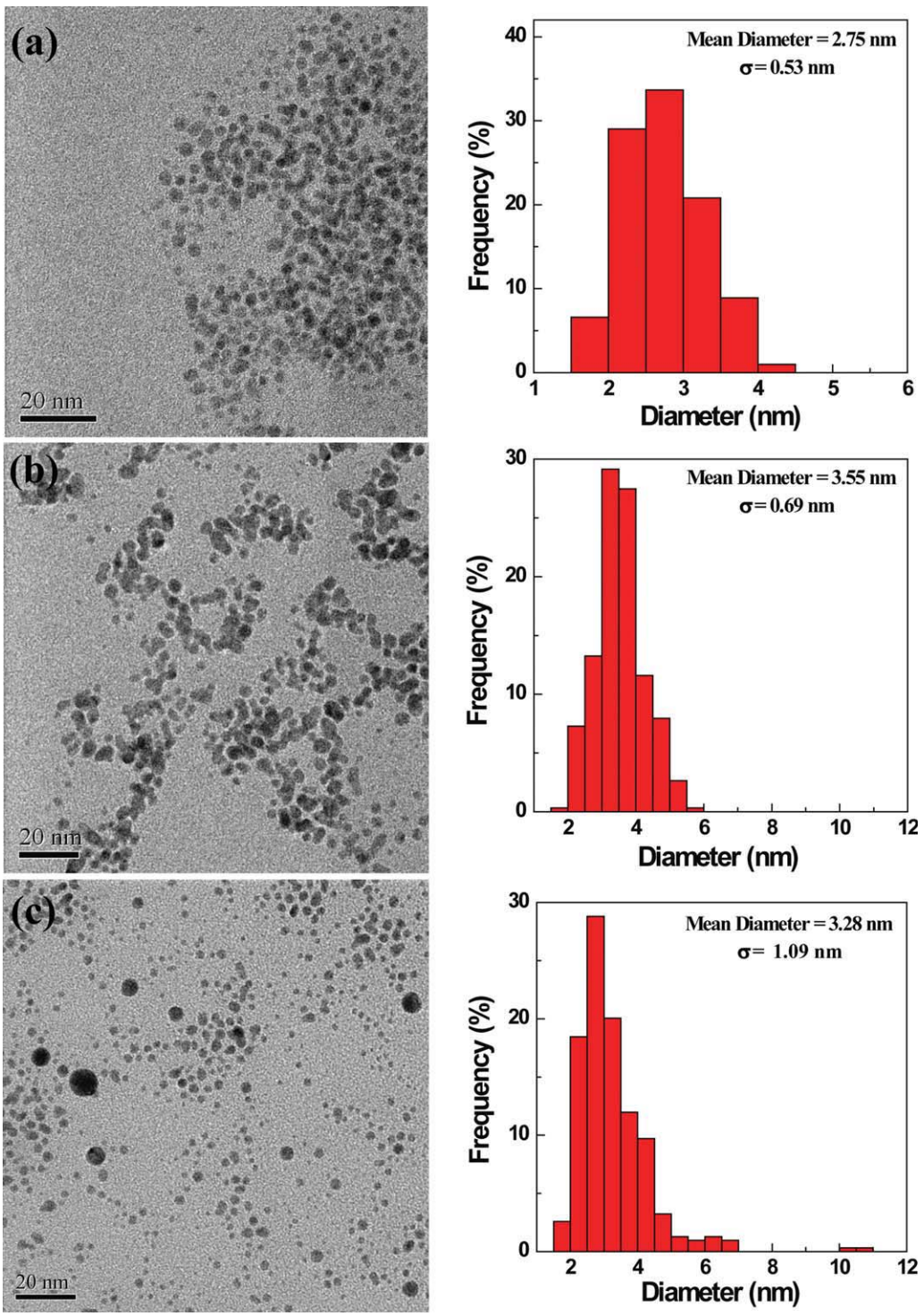

Figure 5 TEM images and size distribution histograms of $(Au^0)_{125}$-G5.NHAc DENPs (a) stored in dialysis liquid, (b) lyophilized with glucose and redispersed in water, and (c) lyophilized without glucose and redispersed in water. σ represents standard deviation. [Color figure can be viewed in the online issue, which is available at wileyonlinelibrary.com.]

with UV–vis spectrometry (Fig. 4). It was clear that for the $(Au^0)_n$-G5.NHAc DENPs with $n \leq 50$, there was nearly no difference for the particles stored in the dialysis liquid or lyophilized with or without glucose; this suggested that the Au DENPs were stable, which was in agreement with literature data.[22,23] For the $(Au^0)_n$-G5.NHAc DENPs with $n \geq 75$, the characteristic SPR peak of the particles stored in dialysis liquid and the particles lyophilized with glucose were similar; this indicated that the addition of glucose before lyophilization effectively preserved the colloidal stability of the redispersed particles.

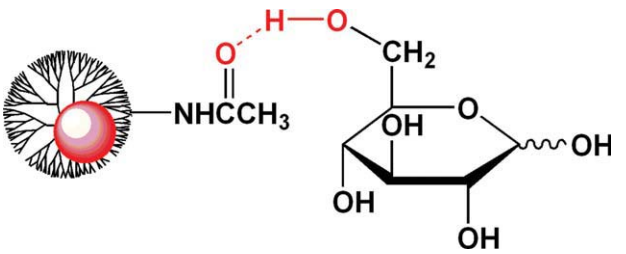

Figure 6 Schematic diagram of $(Au^0)_n$-G5.NHAc DENPs protected by d-(+)-glucose via hydrogen-bonding formation. [Color figure can be viewed in the online issue, which is available at wileyonlinelibrary.com.]

Even after 2 months of storage, the stability of the $(Au^0)_n$-G5.NHAc DENPs ($n \geq 75$) protected by glucose remained identical to those stored in the dialysis liquids when they were redispersed in water, and no aggregation could be found. In contrast, the characteristic SPR peak of the acetylated Au DENPs lyophilized without the addition of glucose had a slight redshift (3–4 nm), which confirmed weak stability or aggregation after the lyophilization process.

The size and morphology of the acetylated Au DENPs under different conditions were further characterized with TEM (Fig. 5). It was clear that the size of the $(Au^0)_{125}$-G5.NHAc DENPs stored in the dialysis liquid and the same particles protected by glucose fell within a relatively narrow range [Fig. 5(a,b)]. In contrast, the size of the $(Au^0)_{125}$-G5.NHAc DENPs lyophilized without the addition of glucose were relatively polydisperse [Fig. 5(c)]. The $(Au^0)_n$-G5.NHAc DENPs protected by glucose possessed good stability in water, PBS buffer, and cell culture medium; this is essential for their application as contrast agents in CT imaging. The protecting role played by glucose is still unclear now. We believe that hydrogen bonding between the hydroxyl groups of glucose and the dendrimer terminal acetamide groups could have been formed, and the glucose-protected Au DENPs may have had enlarged interparticle distance, which significantly inhibited the aggregation of the particles during the lyophilization process (Fig. 6).

Application of the acetylated Au DENPs for CT imaging

Theoretically, gold has a higher X-ray absorption coefficient than iodine because of its higher atomic number and electron density.[37] Our previous work related to Au DENPs prepared with $G5.NH_2$ dendrimers as templates showed that Au DENPs with a size range of 2–4 nm have better X-ray attenuation properties than iodine-based, clinically used contrast agents (e.g., Omnipaque). It was anticipated that the X-ray attenuation properties of the Au DENPs would not change significantly after the dendrimer terminal amines were acetylated.

The X-ray attenuation of the $(Au^0)_{50}$-G5.NHAc DENPs was compared with that of Omnipaque (Fig. 7). With increasing molar concentration of the active element (i.e., Au or iodine), the X-ray attenuation coefficient of both the DENPs and Omnipaque increased. However, the increasing trend of the Au DENPs was much higher than that of Omnipaque. At a molar concentration of 0.1 *M*, the X-ray attenuation of the $(Au^0)_n$-G5.NHAc DENPs was approximately 100% higher than that of Omipaque. The $(Au^0)_n$-G5.NHAc DENPs with other compositions ($n \geq 75$) protected with glucose basically followed the same trend as a function of Au concentration. This suggested that the X-ray attenuation properties of the Au DENPs did not significantly change after the dendrimer terminal amines were acetylated.[26] With the neutral surface charge and improved biocompatibility,[23] the acetylated Au DENPs should have been amenable for CT imaging applications with high contrast efficiency.

To further prove the feasibility of using acetylated Au DENPs as *in vivo* contrast agents for CT imaging, a PBS buffer solution of $(Au^0)_{50}$-G5.NHAc DENPs (500 μL, [Au] = 0.1 mol/L) was intravenously injected into a mouse through a tail vein, and a CT image was collected [Fig. 8(a)]. In the CT image, parenchyma, including muscles and blood vessels, were gray and even dark, whereas bones were white because of their higher density and the resulting stronger X-ray absorption, such as the mouse's

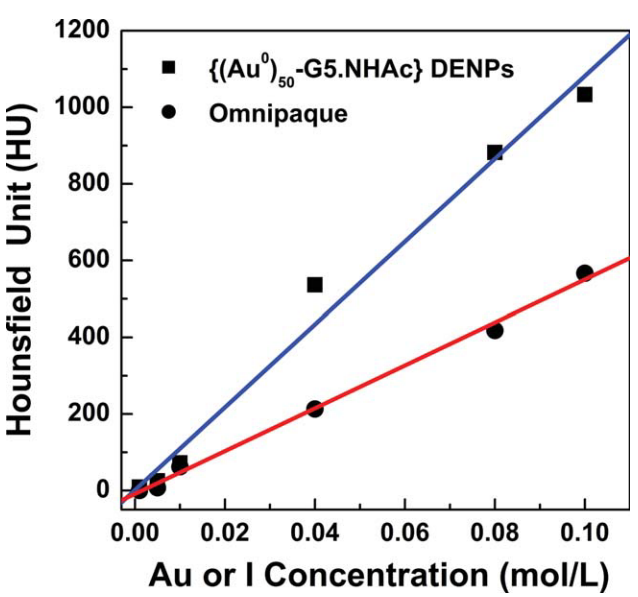

Figure 7 X-ray attenuation (Hounsfield units) of $(Au^0)_{50}$-G5.NHAc DENPs and Omnipaque as a function of the molar concentration of the active element (Au or iodine). [Color figure can be viewed in the online issue, which is available at wileyonlinelibrary.com.]

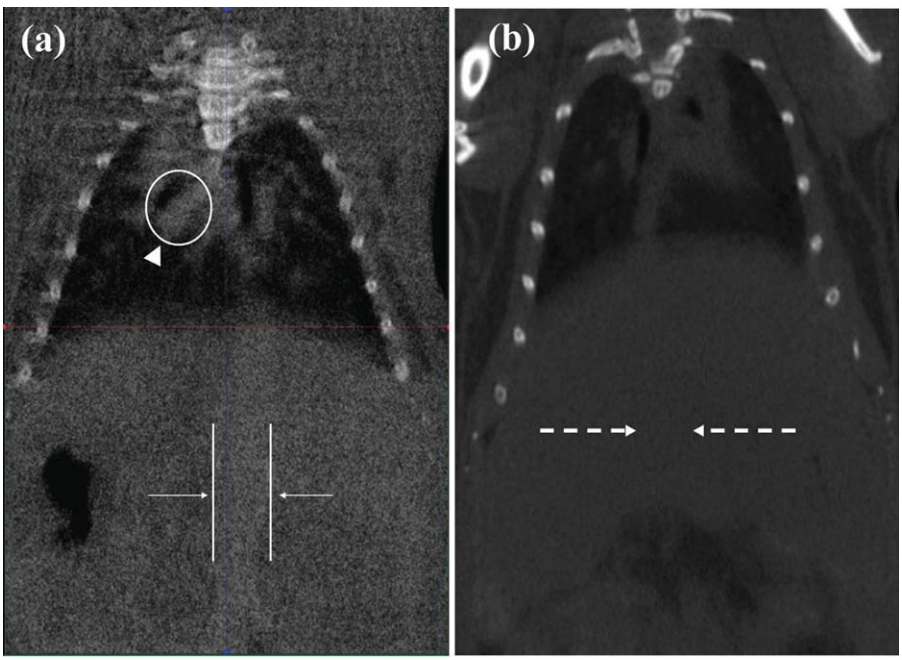

Figure 8 CT image of a mouse intravenously injected with 500 μL of (a) $(Au^0)_{50}$-G5.NHAc DENPs ([Au] = 0.1 mol/L) and (b) Omnipaque ([I] = 0.1 mol/L), [I] denotes the iodine concentration through a tail vein. In part a, the white arrowhead and the white circle indicate the mouse's pulmonary veins, and the white arrows and white lines point to the inferior vena cava of the mouse. In part b, the white dotted arrows point to the inferior vena cava of the mouse, which was undetectable in the CT image.

spondyle in our case. The existence of Au NPs within the parenchyma could be easily visualized in the CT image because of their much higher attenuation coefficient than that of the parenchyma [Fig. 8(a)]. In Figure 8(a), the white arrows and white lines indicate the mouse's inferior vena cava, and the white arrowhead and white circle indicate the pulmonary veins of the mouse, which can be clearly distinguished as a bright strip in the CT image due to the limited diffusion and, hence, localized distribution of $(Au^0)_{50}$-G5.NHAc DENPs. In contrast, the corresponding organs could not be distinguished when Omnipaque with an iodine concentration similar to that of Au of the DENPs was injected under similar conditions [Fig. 8(b)]. This suggests that the acetylated Au DENPs displayed stronger X-ray attenuation and longer circulation times compared with those of Omnipaque. More importantly, mice injected with the $(Au^0)_{50}$-G5.NHAc DENPs were healthy without any signs of illness, similar to the case where Omnipaque was used. The mentioned biocompatibility of the acetylated Au DENPs was just based on an 3-(4,5-dimethylthiazol-2-yl)-2,5-diphenyltetrazolium bromide (MTT) assay of cell viability and a short-term *in vivo* experiment. Long-time observation is strongly required for further clinical trials of the developed Au DENP materials.

CONCLUSIONS

In summary, Au DENPs prepared with G5.NH_2 dendrimers were subjected to an acetylation reaction to neutralize the surface charge of the particles. By varying the Au salt/dendrimer molar ratio, acetylated Au DENPs with a size range of 2–4 nm can be prepared. For further biological applications, we investigated the effect of the storage/processing conditions on the stability of the acetylated Au DENPs. We showed that for acetylated Au DENPs prepared with an Au salt/dendrimer molar ratio equivalent to or higher than 75 : 1, lyophilization significantly weakened the stability of the particles upon redispersion in water. To solve this problem, glucose was added to the dialysis liquid of the acetylated Au DENPs before lyophilization. The addition of glucose significantly preserved the stability of the redispersed particles. X-ray absorption coefficient measurements showed that the attenuation of acetylated Au DENPs was much higher than that of the iodine-based contrast agent at the same molar concentration of the active element (Au vs iodine). Furthermore, we showed that the acetylated Au DENPs enabled *in vivo* CT imaging of mice after intravenous injection. With the unique structural characteristics of the dendrimers, the Au DENPs could be conjugated with various targeting ligands (e.g., folic acid, RGD peptide, antibodies), followed by acetylation to

neutralize the surface charge of the particles.[22,30] We expect that Au DENPs with neutral surface charges can be used as a multifunctional nanoplatform for the CT imaging of tumors. Related work is currently being done in our laboratory.

References

1. Daniel, M. C.; Astruc, D. Chem Rev 2004, 104, 293.
2. Kim, Y. G.; Oh, S. K.; Crooks, R. M. Chem Mater 2004, 16, 167.
3. Li, D. X.; Cui, Y.; Wang, K. W.; He, Q.; Yan, X. H.; Li, J. B. Adv Funct Mater 2007, 17, 3134.
4. Li, D. X.; He, Q.; Cui, Y.; Li, J. B. Chem Mater 2007, 19, 412.
5. Li, D. X.; He, Q.; Cui, Y.; Wang, K. W.; Zhang, X. M.; Li, J. B. Chem Eur J 2007, 13, 2224.
6. Okugaichi, A.; Torigoe, K.; Yoshimura, T.; Esumi, K. Colloid Surf A 2006, 273, 154.
7. Parak, W. J.; Gerion, D.; Pellegrino, T.; Zanchet, D.; Micheel, C.; Williams, S. C.; Boudreau, R.; Le Gros, M. A.; Larabell, C. A.; Alivisatos, A. P. Nanotechnology 2003, 14, R15.
8. Rosi, N. L.; Mirkin, C. A. Chem Rev 2005, 105, 1547.
9. Shenhar, R.; Rotello, V. M. Acc Chem Res 2003, 36, 549.
10. Boisselier, E.; Astruc, D. Chem Soc Rev 2009, 38, 1759.
11. Gobin, A. M.; Lee, M. H.; Halas, N. J.; James, W. D.; Drezek, R. A.; West, J. L. Nano Lett 2007, 7, 1929.
12. Guo, R.; Li, R. T.; Li, X. L.; Zhang, L. Y.; Jiang, X. Q.; Liu, B. R., Small 2009, 5, 709.
13. Huang, X. H.; El-Sayed, I. H.; Qian, W.; El-Sayed, M. A. J Am Chem Soc 2006, 128, 2115.
14. Huang, Y. F.; Sefah, K.; Bamrungsap, S.; Chang, H. T.; Tan, W. Langmuir 2008, 24, 11860.
15. Connor, E. E.; Mwamuka, J.; Gole, A.; Murphy, C. J.; Wyatt, M. D., Small 2005, 1, 325.
16. Shukla, R.; Bansal, V.; Chaudhary, M.; Basu, A.; Bhonde, R. R.; Sastry, M. Langmuir 2005, 21, 10644.
17. Lala, N.; Lalbegi, S. P.; Adyanthaya, S. D.; Sastry, M. Langmuir 2001, 17, 3766.
18. Skrabalak, S. E.; Chen, J.; Au, L.; Lu, X.; Li, X.; Xia, Y. Adv Mater 2007, 19, 3177.
19. Grohn, F.; Bauer, B. J.; Akpalu, Y. A.; Jackson, C. L.; Amis, E. J. Macromolecules 2000, 33, 6042.
20. Scott, R. W. J.; Wilson, O. M.; Crooks, R. M. J Phys Chem B 2005, 109, 692.
21. Shi, X.; Lee, I.; Baker, J. R., Jr. J Mater Chem 2008, 18, 586.
22. Shi, X.; Wang, S. H.; Meshinchi, S.; Van Antwerp, M. E.; Bi, X.; Lee, I.; Baker, J. R., Jr. Small 2007, 3, 1245.
23. Shi, X.; Wang, S. H.; Sun, H.; Baker, J. R., Jr. Soft Matter 2007, 3, 71.
24. Esumi, K.; Suzuki, A.; Aihara, N.; Usui, K.; Torigoe, K. Langmuir 1998, 14, 3157.
25. Crooks, R. M.; Zhao, M. Q.; Sun, L.; Chechik, V.; Yeung, L. K., Acc Chem Res 2001, 34, 181.
26. Guo, R.; Wang, H.; Peng, C.; Shen, M.; Pan, M.; Cao, X.; Zhang, G.; Shi, X. J Phys Chem C 2010, 114, 50.
27. Dendrimers and Other Dendritic Polymers; Tomalia, D. A.; Frechet, J. M. J., Eds.; Wiley: New York, 2001.
28. Tomalia, D. A.; Naylor, A. M.; Goddard, W. A., III. Angew Chem Int Ed Engl 1990, 29, 138.
29. Shi, X.; Wang, S. H.; Lee, I.; Shen, M.; Baker, J. R., Jr. Biopolymers 2009, 91, 936.
30. Shukla, R.; Hill, E.; Shi, X.; Kim, J.; Muniz, M. C.; Sun, K.; Baker, J. R., Jr. Soft Matter 2008, 4, 2160.
31. Majoros, I. J.; Keszler, B.; Woehler, S.; Bull, T.; Baker, J. R. Macromolecules 2003, 36, 5526.
32. Manna, A.; Imae, T.; Aoi, K.; Okada, M.; Yogo, T. Chem Mater 2001, 13, 1674.
33. Alric, C.; Taleb, J.; Le Duc, G.; Mandon, C.; Billotey, C.; Le Meur-Herland, A.; Brochard, T.; Vocanson, F.; Janier, M.; Perriat, P.; Roux, S.; Tillement, O. J Am Chem Soc 2008, 130, 5908.
34. Kattumuri, V.; Katti, K.; Bhaskaran, S.; Boote, E. J.; Casteel, S. W.; Fent, G. M.; Robertson, D. J.; Chandrasekhar, M.; Kannan, R.; Katti, K. V. Small 2007, 3, 333.
35. Kim, D.; Park, S.; Lee, J. H.; Jeong, Y. Y.; Jon, S. J Am Chem Soc 2007, 129, 7661.
36. Popovtzer, R.; Agrawal, A.; Kotov, N. A.; Popovtzer, A.; Balter, J.; Carey, T. E.; Kopelman, R. Nano Lett 2008, 8, 4593.
37. Xu, C. J.; Tung, G. A.; Sun, S. H. Chem Mater 2008, 20, 4167.
38. Takeuchi, Y.; Ida, T.; Kimura, K. J Phys Chem B 1997, 101, 1322.